Power Flows and Mechanical Intensities in Structural Finite Element Analysis

by

Stephen A. Hambric
Applied Mathematics Division (184)
David Taylor Research Center
Bethesda, MD 20084-5000

ABSTRACT

The identification of power flow paths in dynamically loaded structures is an important, but currently unavailable, capability for the finite element analyst. For this reason, methods for calculating power flows and mechanical intensities in finite element models are developed here. Formulations for calculating input and output powers, power flows, mechanical intensities, and power dissipations for beam, plate, and solid element types are derived. NASTRAN is used to calculate the required velocity, force, and stress results of an analysis, which a post-processor then uses to calculate power flow quantities. The SDRC I-deas Supertab module is used to view the final results. Test models include a simple truss and a beam-stiffened cantilever plate. Both test cases showed reasonable power flow fields over low to medium frequencies, with accurate power balances. Future work will include testing with more complex models, developing an interactive graphics program to view easily and efficiently the analysis results, applying shape optimization methods to the problem with power flow variables as design constraints, and adding the power flow capability to NASTRAN.

INTRODUCTION

Structure-borne sound is the vibrational energy which travels through dynamically loaded mechanical systems. This vibrational energy is radiated eventually into an acoustic medium as noise. An example cited by Wohlever and Bernhard[1] is an airplane wing loaded by engine vibrations. The vibrational energy travels along the wing to the fuselage and is radiated as sound into the cabin. Architects face the problem of structure-borne sound in hotels and apartment buildings, where vibrational energy flows through walls and floors, and is radiated as sound into other rooms. This problem is addressed by

Luzzato and Ortola.[2]

Dynamic analyses are performed to solve these problems, which output exorbitant amounts of data. The analyst is then faced with the problem of interpreting the output. Tabular printouts can be analyzed, spectrum plots generated, and deformed shapes plotted, all of which are useful methods of defining the state of a structure. Another way of quantifying the propagation of structure-borne sound is the calculation of power flows. This method will identify the magnitude and direction of the power at any location in a structure, helping an analyst to find the dominant paths of energy flow and the energy sinks for a given problem. The understanding of the paths of energy which flow from a vibration source (such as the engine in the aircraft example) to certain parts of a structure (the cabin for example) would help an engineer to more easily pinpoint and correct vibration problems.

The important terms used in this study are: power flow, which is actually power, or energy flow, but is termed power flow by the scientific community of this field; mechanical intensity, which is power flow per unit area; and power dissipation, which is the time rate of energy dissipated in a structure. Four main methods for identifying dominant power sources and power flow paths are addressed in the literature: experimental methods, statistical energy analysis, the finite element method, and the power flow method.

Experimental solutions are the most common in the literature. The authors of some of these papers[3–7] use multiple transducers and digital signal processing techniques to solve various power flow problems. A common method is the calculation of cross spectral densities, where two accelerometers are placed a known distance apart on a structure, and response spectra are generated for the two measurement locations. The correlation between the spectra is statistically analyzed, and power flows are computed over some range of frequencies. This approach is similar to the two-microphone technique used by acousticians to solve noise propagation problems in fluid media. Once an experimental apparatus is set up, the analyst may easily vary applied loads and loading frequencies. Unfortunately, accuracy problems may occur due to the added weights and inertias of the transducers attached to an experimental structure.

Statistical energy analysis (SEA) is a computational method used to solve energy flow problems in the high frequency domain. A definitive reference on SEA, although now out of print, is the text by R.L. Lyon.[8] A brief summary of SEA follows. Large structures are split into smaller subsystems; a modal density is estimated for each subsystem so the number of modes in a given frequency band can be determined; dissipation loss factors, which relate energy stored to power dissipated, are estimated for the subsystems; and coupling loss factors, which relate differences of modal energy of subsystems to power flow, are assigned to the junctions of the

subsystems. The energy distribution, power flows, and power dissipations are then computed.

SEA is a reasonable way of solving for the average response of structures at high frequencies; however all spatial variations of the power flow field in the substructures remain unknown. A more discrete method must be used to identify specific power flow paths through a structure. Finite element analysis (FEA) may be used for this purpose, but is only cost effective for low to mid-range frequencies, since higher mode shapes are more complex, wavelengths are shorter, and denser finite element meshes are required to model a problem correctly. Mickol and Bernhard[9] succesfully used FEA to identify power flow paths in simple beam and plate structures excited at low frequencies.

Recently, some scientists have proposed a new method to solve for power flows in the middle frequency range. Cuschieri,[10] Nefske and Sung,[11] and Wohlever and Bernhard[1] have been studying this new approach: a finite element analogy where input power is substituted for input force and the power flow field may be solved for directly using a finite element solution.

In this paper FEA is used to solve the power flow problem. For lower modes the method is accurate, models are simple to build and modify using modern modeling software, and analysis results are viewed easily using post-processing graphics packages. Since no commercial software contains a power flow capability, the formulations and computer methods are developed here for NASTRAN.[12] The FEA studies presented in the literature consider only the contribution of flexural wave motion to power flow. Other motion types of power flow, such as axial and torsional, are ignored. In this study, all types of power flow are considered.

First, general methods and formulations for power flows and mechanical intensities, power dissipations, input powers, and output powers are developed for global models, beam elements, plate elements, solid elements, and scalar elements. The required NASTRAN solution, the algorithm of the power flow processor, and the use of I-deas Supertab are outlined. Two test models are analyzed to verify the methods: a simple truss and a beam-stiffened cantilever plate. Finally, based on the results of the test case analyses, conclusions about the method are formed and some thoughts about future directions for work are discussed.

THE FINITE ELEMENT SOLUTION

General Methods

A typical power flow cycle is shown in Fig. 1. The figure shows an arbitrary structure mounted to a connecting structure by a spring and damper coupling. A dynamic load is applied, and energy flows into the structure at the load point. The input power then flows through the structure along multiple

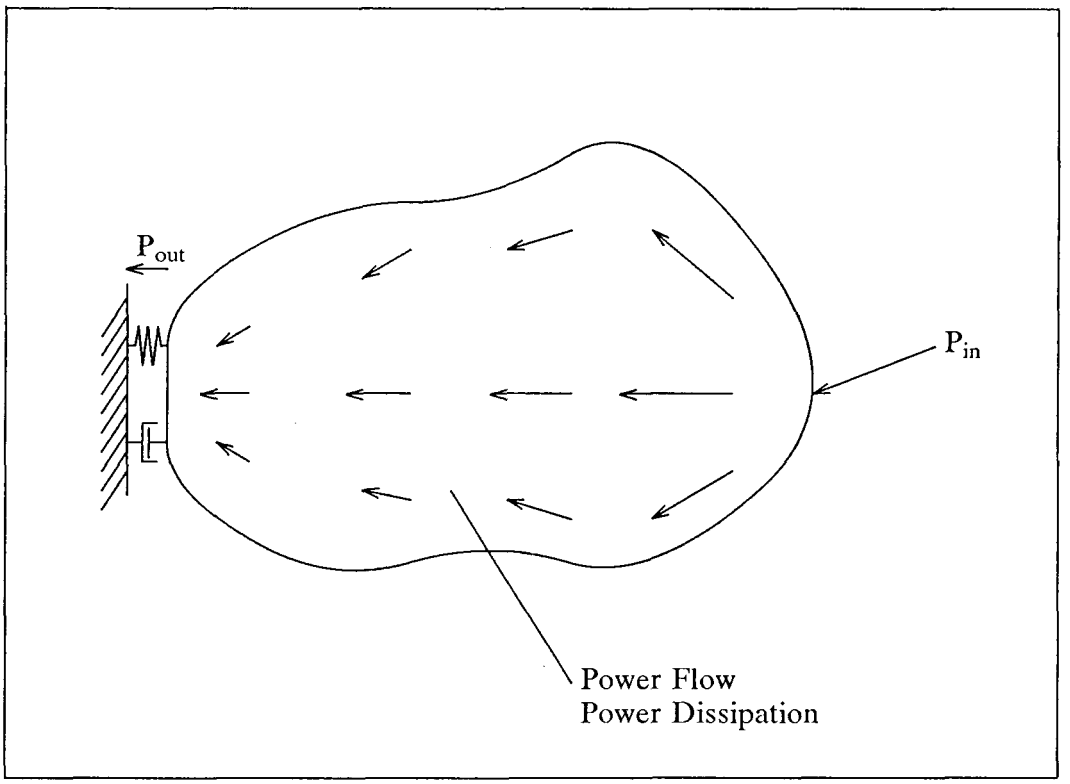

Fig. 1. Sample Power Flow Diagram.

flow paths denoted by arrows, whose lengths represent power flow magnitudes. As the energy flows toward the mounting, it is dissipated by material damping and sound radiation into a surrounding medium, and the flow arrows shorten. The flow and dissipation processes continue until the remaining energy exits the structure through the mounting and flows into the connecting structure. Though only one power entry and exit point is shown in this drawing, multiple loads and mountings may exist. A classic text which describes the flow of structure-borne sound is the book by Cremer, Heckl, and Ungar.[13]

The power flow problem may be solved using NASTRAN. The structure may be modeled using various element types; mountings are modeled using scalar spring, damping, and mass elements; and constraints and loads are directly applied. The steady-state response for the model is solved for a given excitation frequency, and the power flow variables are calculated.

Power Flow and Mechanical Intensity

To calculate power input, power flow, or power output at some location in a given direction, the force in that direction is multiplied by the in-phase

part of the velocity in that direction. For example, a bending moment about the x direction is multiplied by the in-phase part of the angular velocity about the x direction. The power flow at that degree of freedom is the real part of that result. This calculation may be visualized as taking the dot product of the force and velocity phasors to solve for the real part of power.

Multiplying one complex number by the in-phase part of another complex number is the same operation as multiplying the first number by the complex conjugate of the other number. Therefore a general formula for power flow in a structure is

$$\text{Power} = Fv^{*}. \tag{1}$$

Power flow is a complex number. The real part of the calculation is called the active power, and the imaginary part is called the reactive power. The active power is the quantity of interest here.

Mechanical intensity is power flow per unit area, or the stress multiplied by the complex conjugate of velocity. Mechanical intensity is similar to acoustic intensity, which is the pressure in a fluid medium multiplied by the complex conjugate of velocity.

Damping and Power Dissipation

Power may be dissipated in different ways: by material damping, by mountings and surrounding structures, and by radiation as sound. This section discusses the power dissipation due to damping. At this time only material damping is considered in the dissipation process. The effects of sound radiation will be considered in the future.

Power dissipation is calculated differently from power flow and power input. Since power dissipation is the rate of energy dissipation, the energy level of a given element is calculated and multiplied by its damping coefficient. Multiplying the energy dissipation by the angular frequency of excitation gives the power dissipated in that element.

The effects of the material damping coefficient are significant. As the damping coefficient is increased, the power dissipated will increase. If the damping coefficient is zero, no scalar damping elements are applied to the structure, and no sound radiation is considered, power dissipation will be zero and no power flow will exist. This is because, with no damping, forces and velocities will be exactly 90 degrees out of phase, and the in-phase part of velocity is zero. Though this is a physically unrealistic situation, it is one that may occur in a finite element analysis.

To solve for power dissipation, energy dissipation must first be calculated. The energy level in an element is the sum of the element's kinetic energy and potential energy. Since this is a steady-state problem, and the energy is a time-averaged quantity, it may be calculated as twice the kinetic energy:

$$E = mvv^*, \tag{2}$$

where

E = energy,
m = element mass, and
v = velocity.

Power dissipation is then calculated as

$$P_{diss} = 2\pi f \eta E, \tag{3}$$

where

f = rotational frequency, and
η = material damping coefficient.

The ηE term is the energy dissipation, and multiplying by the angular frequency gives the energy dissipation per unit time, or power dissipation. The result will be a real number, since the energy calculation multiplies velocity by its complex conjugate.

The calculation of power dissipation includes the element mass, so the calculation is mesh-dependent. As mesh density increases, element power dissipations decrease. For example, if a beam element were subdivided into two beam elements, the original power dissipation would be split between the two new beams. A way to make the power dissipation calculations mesh-independent would be to divide the results by their respective element masses. At this point, however, the actual power dissipations are calculated because of their importance in checking power balances (see the *Power Balance* section below).

Also, power dissipation is directly related to the mode shapes of an analysis, so areas of large displacements and velocities will be large energy sinks, and nodes (points of near zero displacement) will dissipate almost no power.

Power Input

Power inputs are calculated by multiplying input forces by the complex conjugates of their corresponding velocities. Total input power is calculated as

$$P_{in} = \text{Real}\left[\sum_{i=1}^{n} F_i v_i^*\right], \tag{4}$$

where

i = load point, and
n = number of loads.

This is a global calculation which is independent of element type.

At this time only force inputs are considered. Other load types may input power to a structure, such as displacements, velocities, and accelerations. The calculation of input powers for these load types will be derived in a subsequent paper.

Power Output

Power output is the power that leaves the system through its mountings and enters the connecting system(s). The external system is modeled using spring, damper, and mass elements. These scalar elements must be connected to additional grid points which are grounded. The forces of constraint are combined with the velocities of the grid attached to the scalar element to calculate power output. The power output is calculated as

$$P_{out} = \text{Real}\left[\sum_{i=1}^{n} F_i v_i^*\right], \tag{5}$$

where

i = grounded grid, and
n = number of grounded grids.

Power Balance

The terms described above (power input, power dissipation, and power output) are all used to verify a power balance for a given problem. The power balance equation is

$$P_{in} = \sum_{i=1}^{\#elem} P_{diss} + P_{out.} \tag{6}$$

This is the same equation used in SEA theory. Since P_{in}, P_{out}, and P_{diss} are all calculated independently, if the power balance equation holds, then the power flow solution is correct (assuming the original finite element solution is accurate). This power equilibrium equation is therefore an important check on the power formulations and calculations.

Element Formulations

Beam Elements

Most of the literature in the field of power flow is devoted to beams. The landmark paper by Noiseux[14] described methods of measuring the flexural power flow in beams. Many other authors, such as Verheij,[15] Li,[16] Wohlever and Bernhard,[1] and Nefske and Sung[11] have developed power flow capabilities for beam elements.

All the methods developed, however, consider only flexural power flow. Though flexure is arguably the dominant response in a beam, cases arise where axial and torsional response are important. For this reason, all possible components of power flow will be considered.

Power flow methods for BAR element types are derived below. Either lumped mass or coupled mass solutions may be used. Unfortunately, torsional inertia for the BAR element type is not calculated by NASTRAN. Concentrated mass elements with beam torsional inertias entered as masses must be added to the model at the appropriate degrees of freedom (DOF) to solve for accurate torsional power flows.

Power Flow and Mechanical Intensity. A diagram of the BAR element and its force output conventions is shown in Fig. 2.

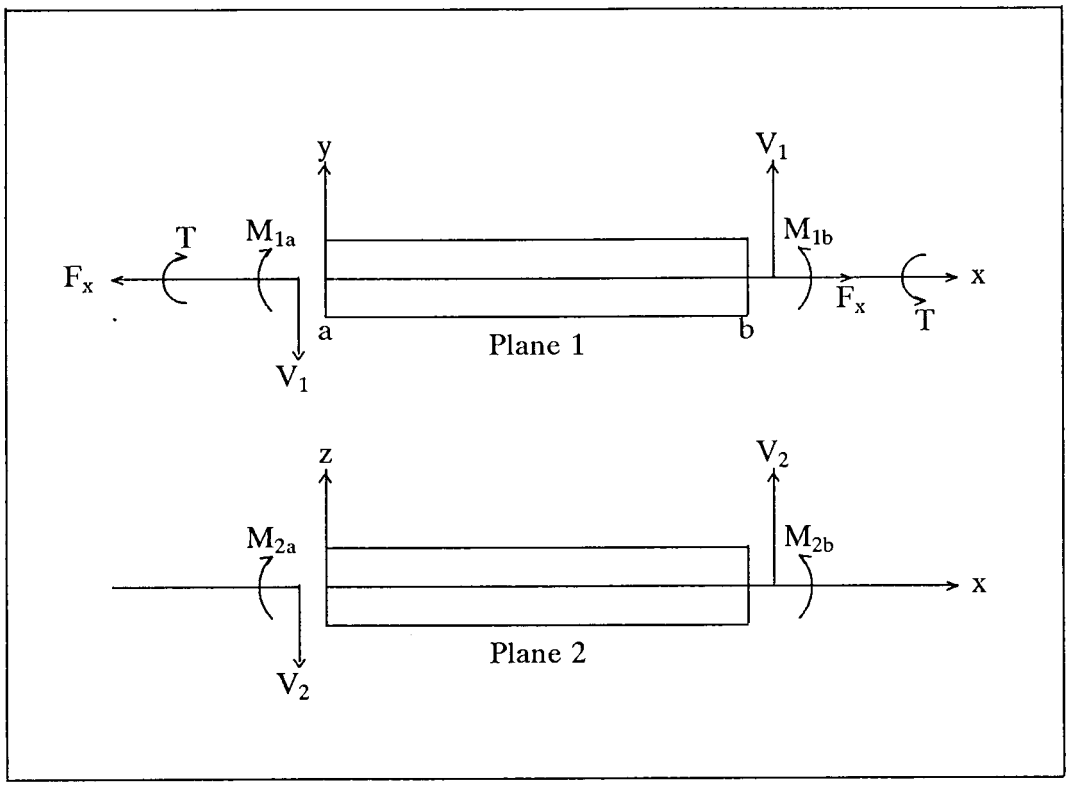

Fig. 2. The BAR Element

Since a beam is a one-dimensional element, energy flows in only one direction: in the local x direction, or along the length of the beam. The total power flow for a beam element is

$$P_x = \text{Real}\,[-(F_x v_x^* + V_1 v_y^* + V_2 v_z^* + T\omega_x^* - M_2\omega_y^* + M_1\omega_z^*)], \tag{7}$$

where

F_x = axial force,
V_1 = shear force in y direction,
V_2 = shear force in z direction,

T = torsion about x,
M_2 = bending moment about y,
M_1 = bending moment about z,
v_i = translational velocities in direction i, and
ω_i = rotational velocities about axis i.

The negative sign in front of the result is due to force and displacement direction conventions for the element. Negative signs appear in the formulations for the plate and solid elements for the same reason. The negative sign in front of the M_2 term is due to the NASTRAN force output convention. In Fig. 2, M_2 is shown as positive in the opposite sense to ω_y. Therefore, $M_2\omega_y^*$ is opposite in sign to the other power flow components.

Velocities are calculated by NASTRAN for each grid point, and beam forces are calculated on an element level. This difference creates a problem, because some way of solving for a power flow on an element level is required. The solution is to solve for a power flow at each grid point, and calculate the average quantity for an element.

Shear, axial, and torsional forces are constant through the element, and are the same for each grid point. Bending moments are calculated at each end of the beam element. Velocities are solved for at a global level, and a coordinate system transformation must be performed to find the velocities at the element level. Since the grid coordinates and beam orientation vector are given, the velocity transformation is straightforward. After power flows at each element end are calculated, they are averaged to give an element power flow. Power flows are then transformed back to NASTRAN's basic coordinate system.

Mechanical intensity is power flow per unit area, and since all the power flow in a beam is along the local x axis, intensity is simply the total power flow divided by the beam's cross sectional area.

Two important observations may be made about power flow in beam elements. Since power flow is one-dimensional in beams, it is independent of mesh variations. Increasing mesh density or varying the mesh pattern will not affect greatly the power flow results (assuming the mesh is dense enough to model accurately the mode shapes of the solution). Also, since power flow is dependent on element force quantities that are discontinuous across element boundaries (axial and shear forces, torsion), the power flow and mechanical intensity quantities are not continuous across beam element boundaries.

Power Dissipation. The energy of a beam element includes both translational and rotatory terms, and is calculated as

$$E = m(v_x v_x^* + v_y v_y^* + v_z v_z^*) + I_{xx}\omega_x\omega_x^* + I_{yy}\omega_y\omega_y^* + I_{zz}\omega_z\omega_z^*, \quad (8)$$

where

m = element mass,

I_{yy}, I_{zz} = mass moments of inertia about cross section,
I_{xx} = polar mass moment of inertia about beam axis,
v_i = local translational velocities in direction i, and
ω_i = local rotational velocities about axis i.

For a lumped mass formulation, the energy terms are calculated at the element centroid; for a coupled mass formulation, they are calculated at the beam ends and averaged. The element energy is then multiplied by $2\pi\eta f$, as in Eq. 3, to yield power dissipation.

The rotational inertial energies are generally small. However, if the beam lengths are long with respect to the cross section, the mass moments of inertia become important. In the case of torsion, where the only large displacement is rotation about the beam's axis, the polar mass moment of inertia term dominates the energy calculation.

Plate Elements

Since the beam element formulation included all components of power flow, power flow capabilities for QUAD elements (QUAD2 and QUAD4), which consider both flexural and membrane effects, are developed.

The literature concerning plate elements is growing, and publications by Mickol and Bernhard,[1] Williams et al,[17] Koshiroi and Tateishi,[18] Noiseux,[13] Fahy and Pierri,[19] and Cuschieri,[20] investigate mechanical intensities and power flows through plate structures. Similar to the literature for beams however, most approaches consider only flexural effects.

Power Flow and Mechanical Intensity. A diagram of a QUAD element and its force and stress output conventions is shown in Fig. 3. The quadrilateral element is two-dimensional, and power may flow in the local x and y directions. The power flow in the x direction is calculated as

$$P_x = \text{Real}\,[-(V_x v_z^* - M_x \omega_y^* + M_{xy}\omega_x^* + F_x v_x^* + F_{xy} v_y^*)]; \tag{9}$$

the power flow in the y direction is

$$P_y = \text{Real}\,[-(V_y v_z^* + M_y \omega_x^* - M_{xy}\omega_y^* + F_y v_y^* + F_{yx} v_x^*)],$$

where

V_x, V_y = transverse shear forces,
M_x, M_y = bending moments,
M_{xy} = twisting moment,
F_x, F_y = membrane forces,
F_{xy}, F_{yx} = membrane shear,
v_i = local translational velocities in direction i, and
ω_i = local rotational velocities about axis i.

The negative signs in front of the $M_x\omega_y^*$ and $M_{xy}\omega_y^*$ terms are due to the

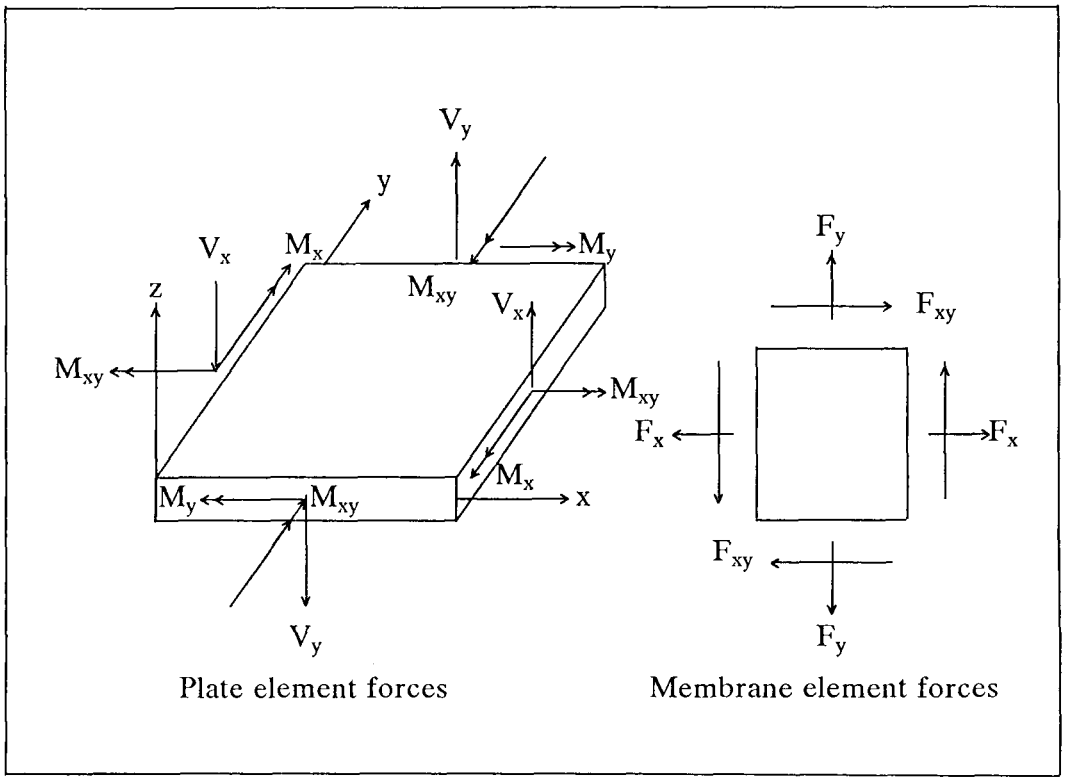

Fig. 3. The QUAD Element

NASTRAN force output convention. These bending moments are opposite in sense to their corresponding rotational velocities.

As in the case of the beam elements, grid velocities must be transformed to the local element coordinate systems to be used in the power flow calculations. After the calculations, the power flow vectors are transformed back to NASTRAN's basic coordinate system.

The above formulation should work for the QUAD2 and QUAD4 element types. Unfortunately, the QUAD4 has not been fully implemented for complex analysis yet, so only the QUAD2 may be used. This is unfortunate, since the QUAD2 is not an isoparametric element, and its membrane performance is poor. In fact, NASTRAN does not calculate membrane forces for the QUAD2, so they must be deduced from the membrane stress outputs.

Calculating membrane forces involves approximating the element's local dx and dy lengths, which combined with the plate thickness will give dA values in the local x and y directions. Multiplying these "side areas" by the stresses

will give approximations for the membrane forces. All this additional calculation introduces more error into a membrane formulation which is already poor. If an element is greatly distorted, the membrane results could be completely incorrect.

Finite element meshes for the QUAD2 must be therefore as uniform as possible, since the element is not isoparametric. Also, if membrane effects are dominant in an analysis, the results will be suspect. When the NASTRAN implementation of the QUAD4 is complete, the QUAD4 element will be used.

The mesh dependence of power flow for QUAD elements has not yet been determined.

To calculate mechanical intensities, P_x and P_y are divided by the estimated side areas.

Power Dissipation. The energy of a QUAD element, considering only scalar mass terms, is

$$E = m(v_x v_x^* + v_y v_y^* + v_z v_z^*), \tag{10}$$

where

m = element mass, and
v_i = local translational velocities in direction i.

Element energies are multiplied by ηf to calculate power dissipations. Power dissipation terms are calculated at each grid point and averaged to solve for the element dissipation. This calculation is mesh-dependent, since power dissipation is directly related to element mass.

Solid Elements

Since literature in the power flow field is largely from the experimental sector, solid elements are generally not considered. An experimentalist cannot place a measuring device inside the material of a solid structure. The paper by Pavic,[7] however, describes a method for measuring structural surface intensity. His method, which involves placing transducers on various surfaces of a machinery system to measure two-dimensional mechanical intensities, may be extended to three dimensions. Since a finite element code has no restrictions on making "measurements" internal to a structure, mechanical intensities may be calculated throughout a solid model.

Power Flow and Mechanical Intensity. For the BAR and QUAD elements, force output is given by NASTRAN. For solid elements, stress output is given at grid points and at the element centroid. Pavic[7] uses stresses and velocities in his formulation of structural surface intensities. His formulas for mechanical intensities, extended to three dimensions, are

$$
\begin{aligned}
I_x &= \text{Real}\,[-(\sigma_x v_x + \tau_{xy} v_y + \tau_{xz} v_z)], \\
I_y &= \text{Real}\,[-(\sigma_y v_y + \tau_{yx} v_x + \tau_{yz} v_z)], \\
I_z &= \text{Real}\,[-(\sigma_z v_z + \tau_{zx} v_x + \tau_{zy} v_y)],
\end{aligned} \tag{11}
$$

where

I_x, I_y, I_z = global mechanical intensities,
$\sigma_x, \sigma_y, \sigma_z$ = normal stresses,
$\tau_{xy}, \tau_{yz}, \tau_{xz}$ = shear stresses, and
v_i = global translational velocities in direction i.

Since element stresses are given in the basic coordinate system, the velocities do not have to be transformed to element coordinate systems as they were for the BAR and QUAD element types. Calculations are made at each grid point and averaged to calculate the element mechanical intensity.

At this point, no attempt is made to compute power flows using the mechanical intensity results. Although the intensity vector is defined, the problem of finding element face areas in the x, y, and z directions remains.

This formulation is valid for any solid element in NASTRAN, including the linear, parabolic, and cubic isoparametric solid elements. Unfortunately, the complex stress output for each of these element types is incorrect. The stress results in the OESC1 data block are wrong, and when they are passed to the output file processor (OFP) module, errors result in the output file. These errors appear to be related to data types, since asterisks appear in the grid point field of the NASTRAN output file.

The errors associated with the isoparametric elements restricts the usable element types to the HEXA2, which is a superposition of ten tetrahedron elements. As was the case for the QUAD elements, when the NASTRAN errors are fixed, the higher level elements will be used.

The mesh dependence of mechanical intensity for solid elements has not yet been determined.

Power Dissipation. The power dissipation calculations are the same as those for the QUAD elements (Eq. 10). Only mass and translational velocity terms are considered. Power dissipation terms are calculated at each grid point and averaged. Again, since the element mass is directly related to the element energy, power dissipation is mesh-dependent.

Scalar Elements

Scalar elements may be used to simulate mountings and structures connected to the finite element model. ELASi and MASSi elements may be used to model stiffness, damping, and mass effects. These elements may be important for certain analyses, such as when a structure is not rigidly mounted. In certain cases, power may flow out of a structure into an isolator, which will

absorb much of the energy, or into a surrounding medium. The accurate modeling of boundary conditions must therefore include scalar element types.

Power Flow, Intensity, and Dissipation. Power flows and power dissipations are not measured in scalar elements, but the presence of external stiffnesses, dampers, and masses may significantly affect the results in the structural element types.

Computer Methods

A flow chart of the solution process is shown in Fig. 4.

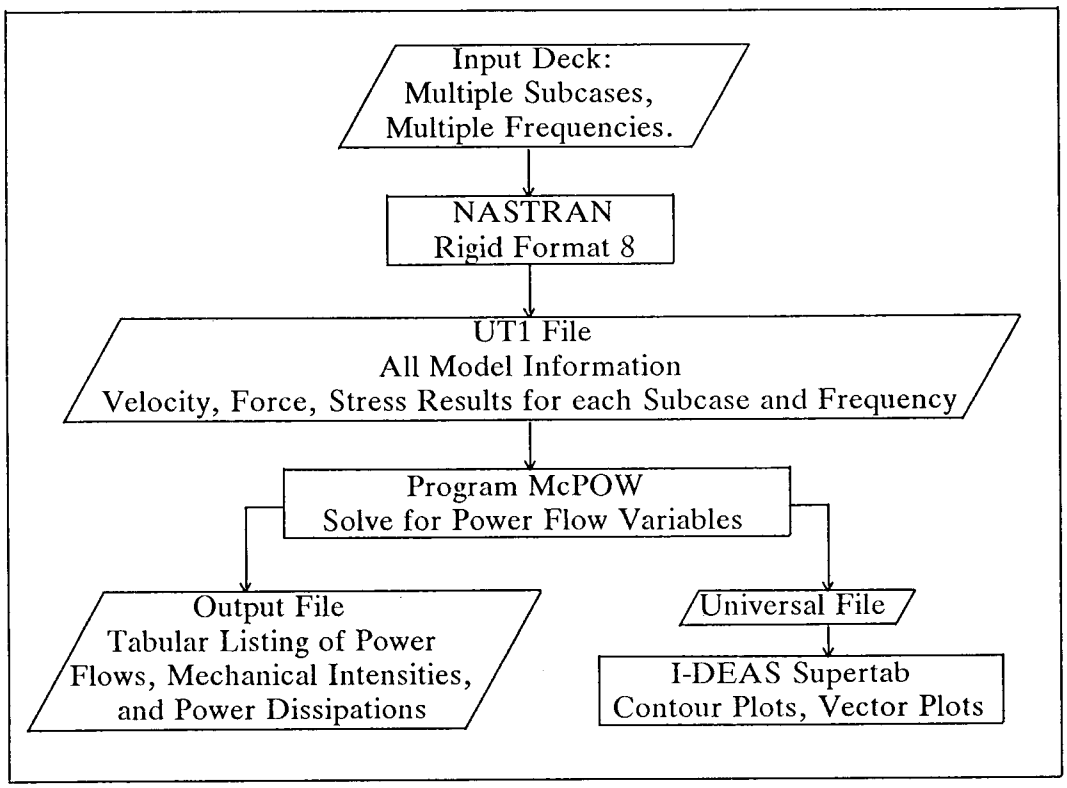

Fig. 4. Power Flow Solution Process

NASTRAN's Rigid Format 8 (Direct Frequency Response) is used to solve a given problem for any combination of load cases and excitation frequencies. The model information and problem solution output are written to a UT1 file, which is used as input to the McPOW (Mechanical POWer) program. After the power computations, power flows, mechanical intensities, and power dissipations are written to two output files. One file contains a tabular listing of the power flow results; the other file is formatted as input to the I-DEAS Supertab[21] post-processor, which is used to interpret visually the results.

C-4

NASTRAN Solution

Before running Rigid Format 8, an eigenvalue extraction (Rigid Format 3) can be performed on the model to determine the resonant frequencies and their corresponding mode shapes. Power flows can then be measured at response peaks, and the dominant type of power flow, such as flexural or axial, can be predicted by examining the mode shapes.

Several data blocks must be written to the UT1 output file for the McPOW program. The following ALTER statements are put in the Executive Control Deck:

```
$
$ THE FOLLOWING STATEMENTS CORRESPOND TO THE 1987,88
$ VERSIONS OF COSMIC NASTRAN, RF8
$
ALTER 23$                                   AFTER THE TA1 MODULE
OUTPUT2 CASECC,EST,MPT,EQEXIN$
ALTER 135$                                  AFTER THE SDR2 MODULE
OUTPUT2 OPPC1,OESC1,OEFC1,OUPVC1$
ENDALTER$
```

In the above alter, the CASECC data block contains case control information, the EST data block holds element information, the MPT data block contains material properties, and the EQEXIN data block holds grid and SIL (Scalar Index List) information. The OPPC1 data block contains the applied forces, the OESC1 data block lists the element stresses, the OEFC1 data block holds element forces, and the OUPVC1 data block contains grid point velocities.

To ensure that all the required data are in the data blocks, the following output requests must be made in the case control deck:

```
FORCE(PHASE)=ALL
STRESS(PHASE)=ALL
VELOCITY(PHASE)=ALL
OLOAD(PHASE)=ALL
```

The capability to calculate power flows for sets of elements will be implemented later.

Power Flow Algorithm

The program McPOW is composed of four main sections: the model information section, the NASTRAN output section, the power flow calculation section, and the output section.

The model information section simply reads the CASECC, EST, MPT, and EQEXIN data blocks from the UT1 file. The NASTRAN output section reads the OPPC1, OESC1, OEFC1, and OUPVC1 data blocks and assigns forces and stresses to element variables, velocities to grid points, and input loads to grid points.

The power flow calculation section first calculates input powers using the input loads and corresponding grid velocities. Next, grid velocities are assigned to elements. Power flows, mechanical intensities, and power dissipations are then calculated using element forces, stresses, and the velocities of the element grids.

The output section writes power flow information to two files. The first contains a tabular listing of the solution variables for each subcase and frequency; the second is a data file in I-DEAS Universal file format.

Post-Processing

The user may analyze the power flow output in two ways: by inspecting the listed output, or using I-DEAS Supertab's post-processor to draw contour plots and arrow plots. Analyzing the tabular output is a good way to check power balances. Power input is equal to power dissipated plus power output. However, to visualize the entire power flow solution in any reasonably complex geometry, a good graphics post-processor is required.

Color contour plots can be used to display power flow magnitudes and power dissipations. Power flow, however, is a vector, and arrow plots are needed to display the direction of the flow. Other authors, such as Heckl,[22] and Koshiroi and Tateishi,[18] have used arrow plots to show power flows in plate structures. An alternative unavailable in I-DEAS Supertab is a combination of a contour and arrow plot, which would illustrate magnitude and direction.

TEST CASES

The test problems illustrate the use of beam, plate, and scalar elements. The QUAD4 and solid elements have not been tested yet.

Simple Truss

Problem Statement

A diagram of a simple truss is shown in Fig. 5. The truss members are constructed of three different types of cross sections. The model was attached to ground at its top and bottom by springs and dampers in all six DOF. The scalar elements simulated the effects of fasteners and the surrounding structure(s). An end load was applied in all six DOF over a range of frequencies. The properties of the two W type sections are given in civil engineering handbooks.

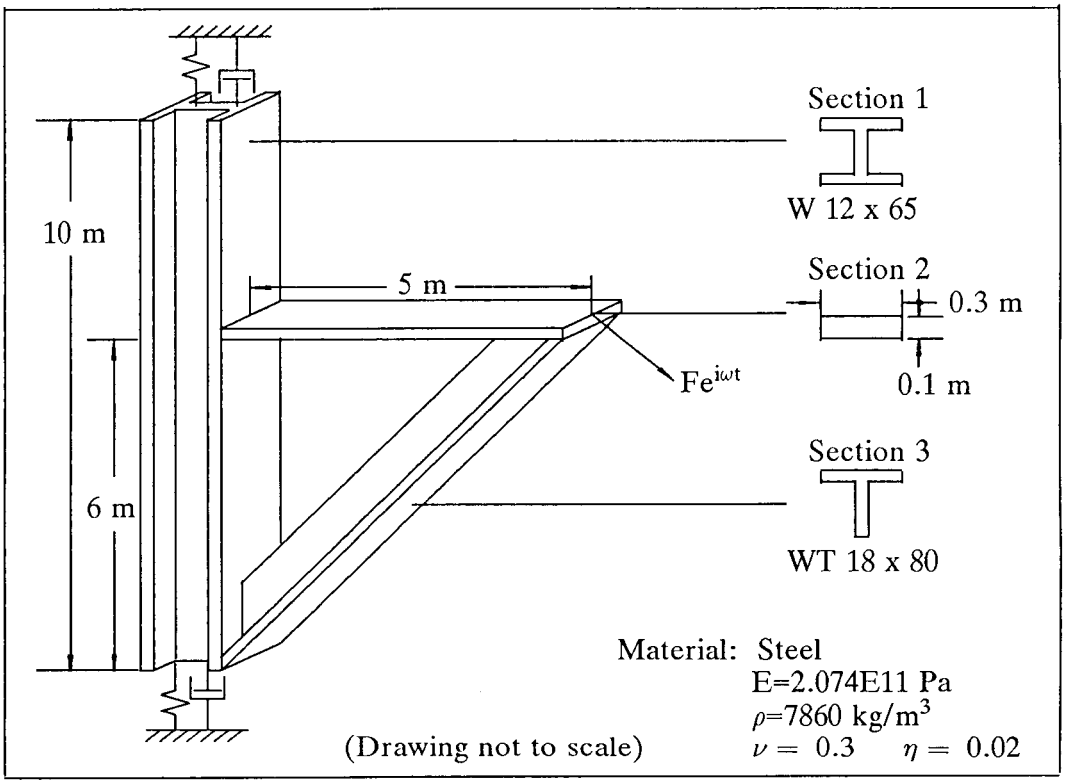

Fig. 5. Simple Truss Problem

The finite element model consisted of 74 BAR elements, with each beam section having a different mesh density. Section 1 was modeled with 40 elements of 0.25 m length, Section 2 consisted of 10 elements of 0.5 m length, and Section 3 was made up of 24 elements of about 0.325 m length. For the scalar elements, spring constants were set at about 100 to 1000 times the stiffness of the members at the appropriate DOF; and the damping constant was set at ten times the material damping constant, or 0.2. This model is a good general test of the power flow methods outlined above, since it has a varying mesh density and the three sections have different beam properties.

Results

The first analysis performed on the model was an eigenvalue extraction (Rigid Format 3). Although there is damping in the model, and the modes are actually complex, real modes may be calculated to estimate the resonances. The first 50 modes ranged in frequency from 1.87 Hz to 174 Hz, with the three members experiencing different types of motion in each mode (i.e., axial, flexural, or torsional), showing the need for the calculation of all types of power flows in beams.

The end load was then applied for frequencies ranging from 1 to 100 Hz, with a resolution of 1 Hz. The plot shown in Fig. 6 shows the response of section three at 100 Hz, or the 29th mode of the truss. The right end of the plot is the loading point, and the left end is the junction with Section 1 and the mounting at the bottom. Both power flow and power dissipation are plotted. Power flow decreases as it propagates along the beam due to power dissipation. Power dissipation oscillates from low to high points, approximating the mode shape of the beam. When dissipation is large, power flow slopes downward; when dissipation is small, power flow remains level.

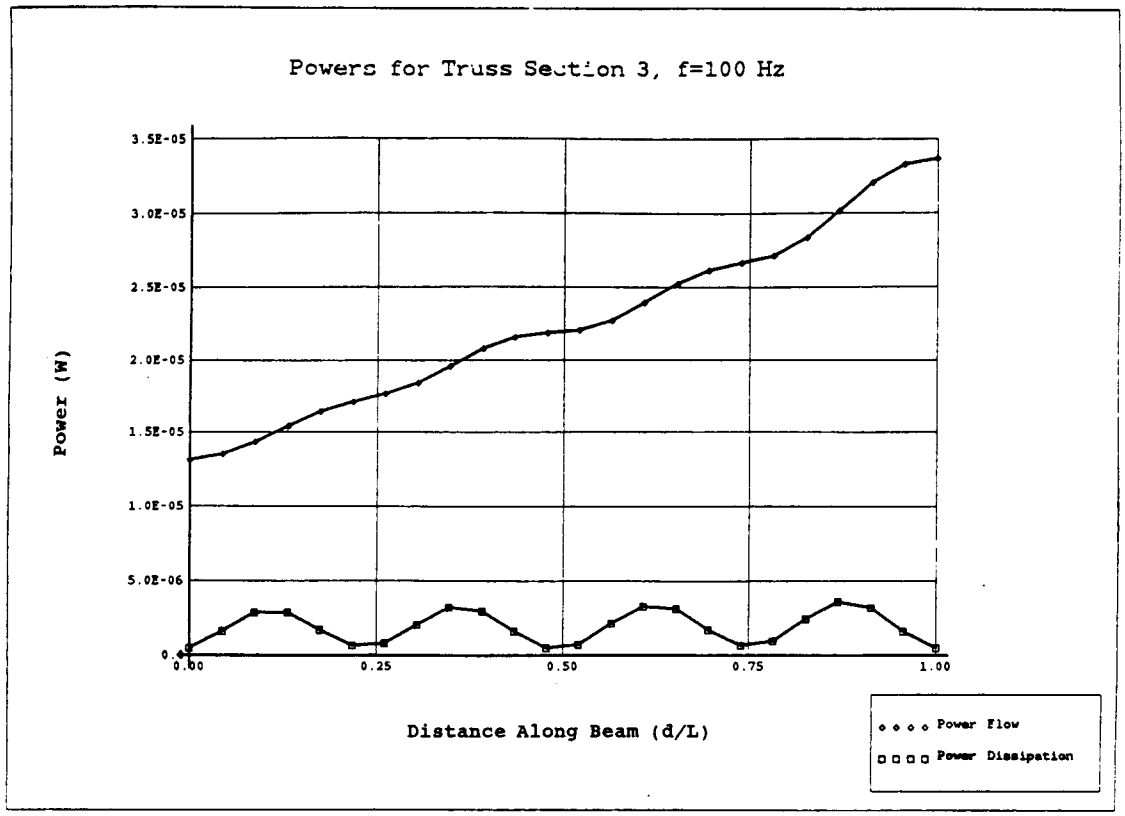

Fig. 6. Power Flows and Dissipations for a Single Frequency

The type of plot shown in Fig. 6 is an effective method of displaying the power flow response for a specific case; however spectra plots are required to illustrate the responses over the entire frequency range. An additional set of plots is shown in Fig. 7 and consists of four plots showing power flow at different locations on each of the truss sections. Section one is split into two graphs: graph one is for the top half of the beam, and graph two is for the bottom half.

Power flows are plotted for three distances along each member: at the beginning, middle, and end (d/L = 0.0, 0.5, and 1.0 respectively). For the top and bottom halves of Section 1, the beginning of the section is at the joint with

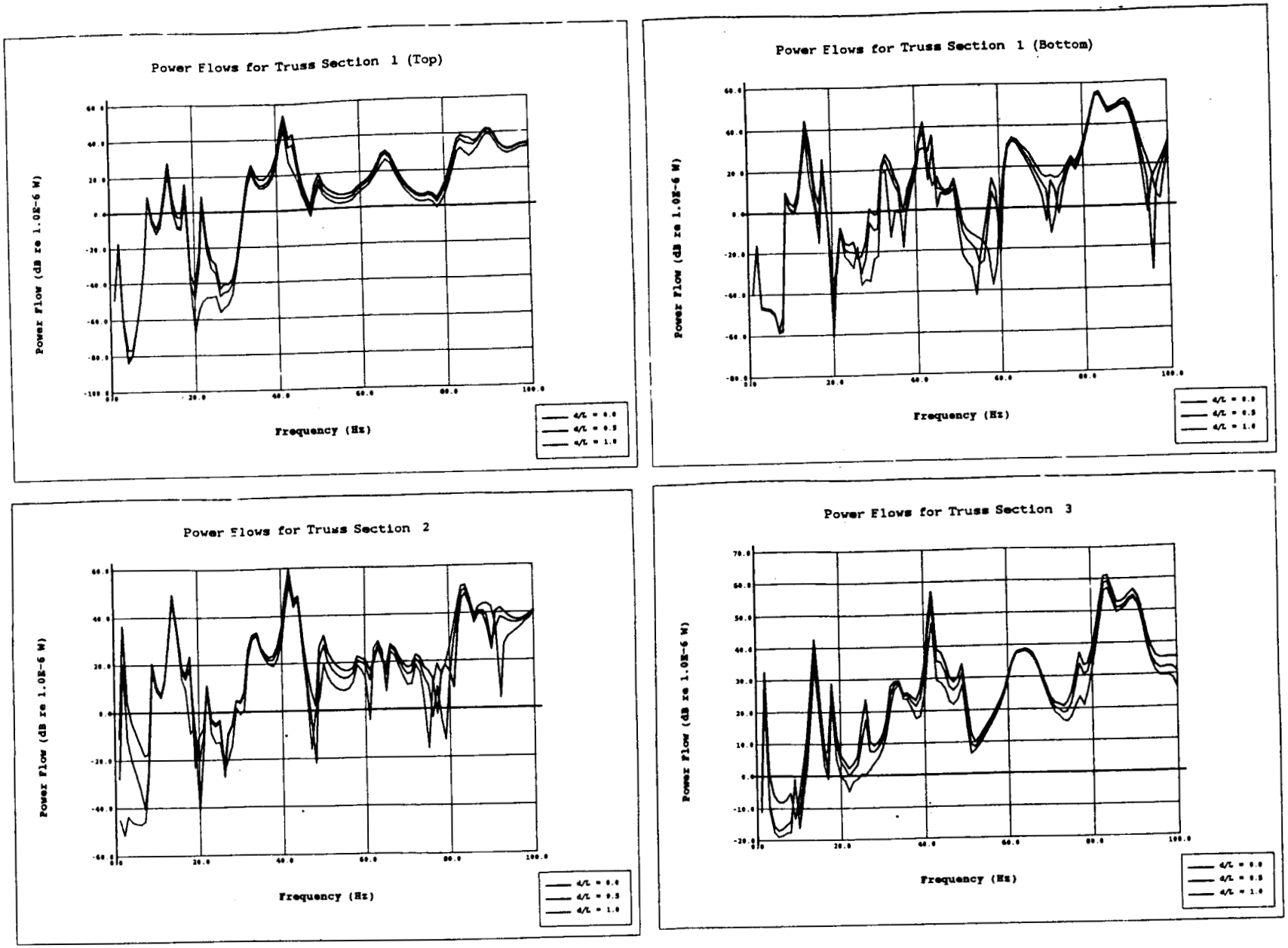

Fig. 7. Spectrum Plots of Power Flows for Truss Sections.

Section 2; for Sections 2 and 3, the beginning of the member is at the load point.

The expected response is a relatively uniform lowering of each curve as power flow progresses from beginning to end along each beam. This is indeed the case for some frequencies. However, at some joints, such as the junction of Sections 1 and 2, and the junction between Sections 1, 3, and ground, power flows in ways that are less intuitive. As a result, some of the plots "cross over" each other and power flow increases from beginning to end. Fig. 8 contains three power flow diagrams which show some of the ways that power may flow through the truss model in this analysis.

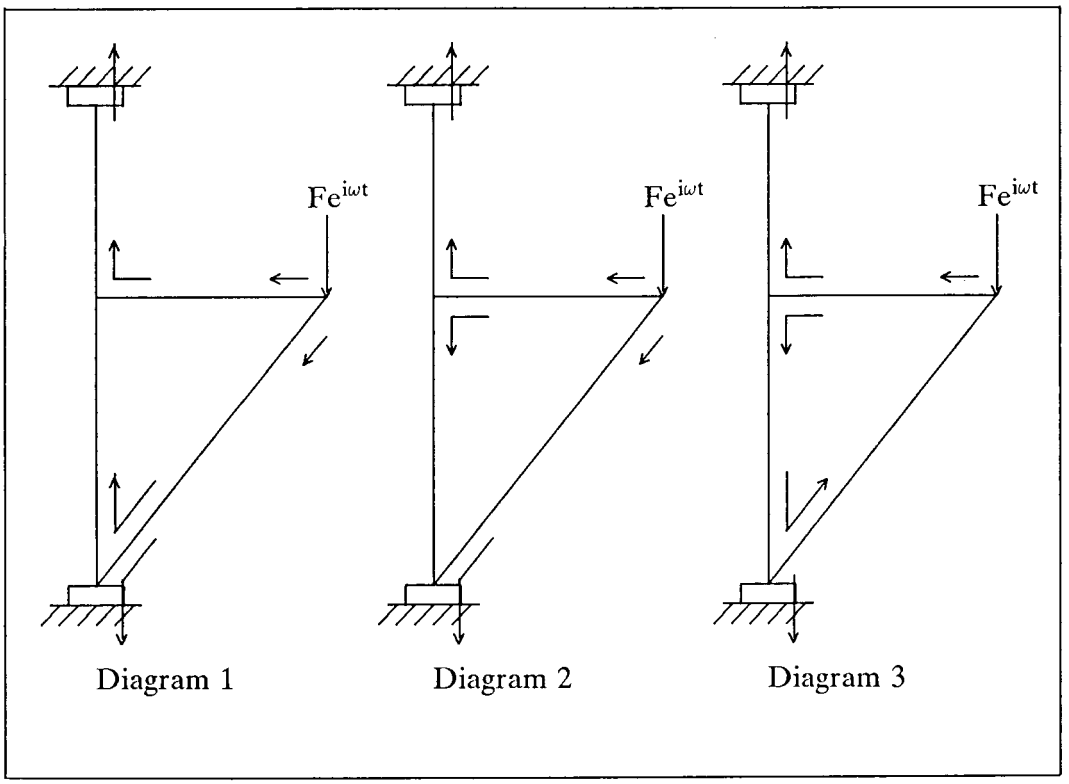

Fig. 8. Power Flow Diagrams for Truss Problem

Diagram 1 shows power entering Sections 2 and 3 at the load points and flowing out toward Section 1. At the junction of Sections 1 and 2, the power flows from Section 2 into the upper half of Section 1. At the junction of Sections 1 and 3, power flows from Section 3 into the scalar elements connected to ground and into the bottom half of Section 1. Power then flows from the bottom of Section 1 to the top of Section 1, where it then flows up to the scalar elements at the top and out of the model.

Diagram 2 shows a similar case, but with two differences. At the junction of Sections 1 and 2, power from Section 2 flows into the top and bottom halves of Section 1; and at the junction of Sections 1 and 3, power flows only into ground.

In Diagram 3, power is input only into Section 2, and flows into the top and bottom halves of Section 1. The power in the bottom half of Section 1 flows down to the junction of Section 1, Section 3, and ground, where some power flows out of the model and some flows up into Section 3.

The cases shown in Diagrams 1 and 2 are the most common based on examination of the printed output. Other possibilities exist, but do not occur often for the range of frequencies analyzed. The type of power flow diagram which occurs for a given frequency may be found by looking at the plots in Fig. 7. When power flow increases travelling from d/L = 0.0 to d/L = 1.0, then power has entered the beam at d/L = 1.0. When power flow decreases travelling from d/L = 0.0 to d/L = 1.0, then power has entered the beam at d/L = 0.0.

Response peaks in the graphs shown in Fig. 7 correspond to different types of motion in each section. Some peaks represent flexural motion, some are due to axial response, and some are torsional in nature. A power flow algorithm which considers only flexural response would give incorrect answers to this problem.

Power balances ($P_{in} = P_{out} + \sum P_{diss}$) were reasonably accurate across the frequency band, with small errors at frequencies of low response. It is uncertain which quantities are in error (P_{in}, P_{out}, or P_{dis}) for these cases, however the errors are of little consequence with respect to the calculations at higher responses. Power flows at the truss joints balanced as well. A calculation similar to Kirchoff's current law can be made, with power flows in the BARs connected to the junctions analagous to currents.

Beam-Stiffened Cantilever Plate

The analysis of ribbed stuctures combines the power flow methods for beams and plates. Nilsson[23] used SEA methods to predict the transmission of structure-borne sound through ribbed plate models. Here, FEA is used to calculate the low frequency response of a beam stiffened cantilever plate.

Problem Statement

A diagram of the model is shown in Fig. 9. Similar to the truss model, the cantilever plate model was attached to ground at its end by springs and dampers in all six DOF. The scalar elements simulated the effects of fasteners and the surrounding structure(s). A uniform end load was applied in the axial, transverse shear, and bending directions. A 12 x 30 mesh of QUAD2 elements was used to model the plate and two sets of 30 BAR elements modeled the stiffeners. The BAR elements were offset relative to the plates.

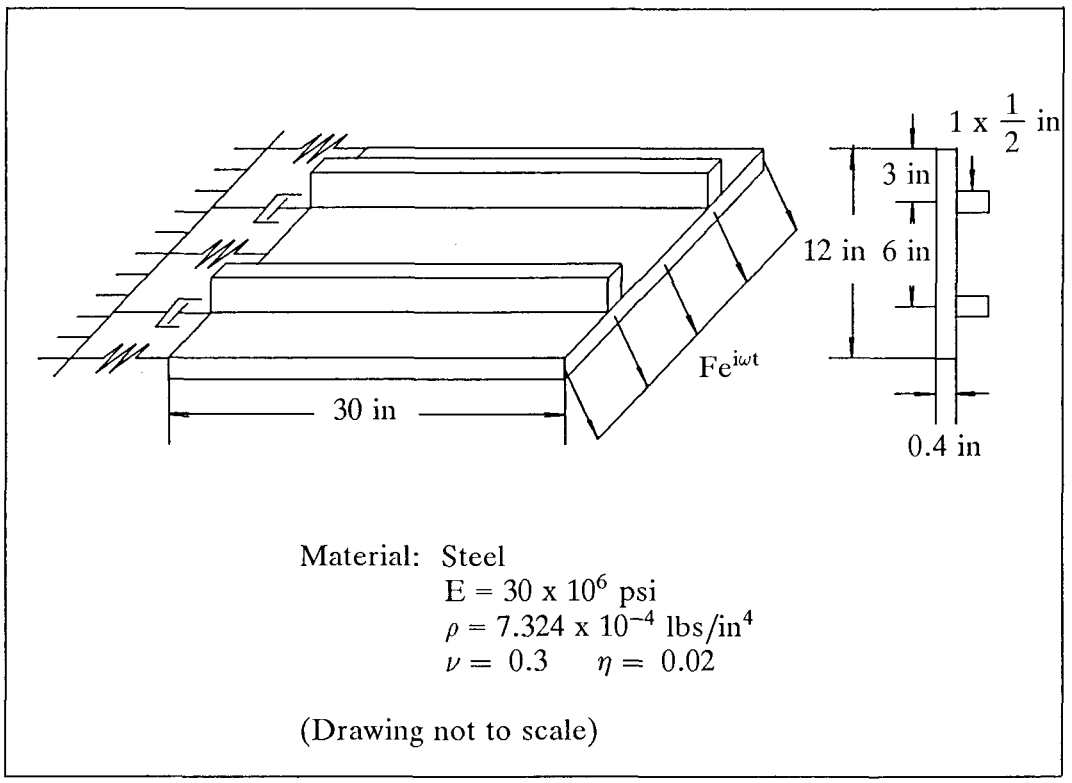

Fig. 9. Beam-Stiffened Cantilever Plate Problem

For the scalar elements, spring constants were set at about 100 to 1000 times the stiffness of the members at the appropriate DOF; and the damping constant was set at ten times the material damping constant, or 0.2.

This model illustrates the power flow capability for plate elements, and helps further test the beam element formulation. Also, the power balance equation is checked for the case of multiple element types in a model; the total power dissipation in the beams plus the total power dissipation in the plates must match the difference of power input and power output.

Results

An eigenvalue extraction of the model showed the first 25 natural frequencies ranging from 15 to 2,122 Hz. Loads were applied to the model for a frequency range of 15 to 465 Hz with a resolution of 15 Hz.

A plot of power flows in one of the beam stiffeners over the frequency range is shown in Fig. 10. Since the model and the loading function are symmetric about the center of the plate, power flows through both beam

stiffeners are the same. Curves are graphed for three locations along the beam, with d/L = 0.0 at the load point. Only two significant resonances appear in the plot; one peak occured at 75 Hz, and the other at about 240 Hz. Although the eigenvalue analysis of the problem predicts other resonant frequencies in this analysis range, their effects are likely felt in the plate section of the model.

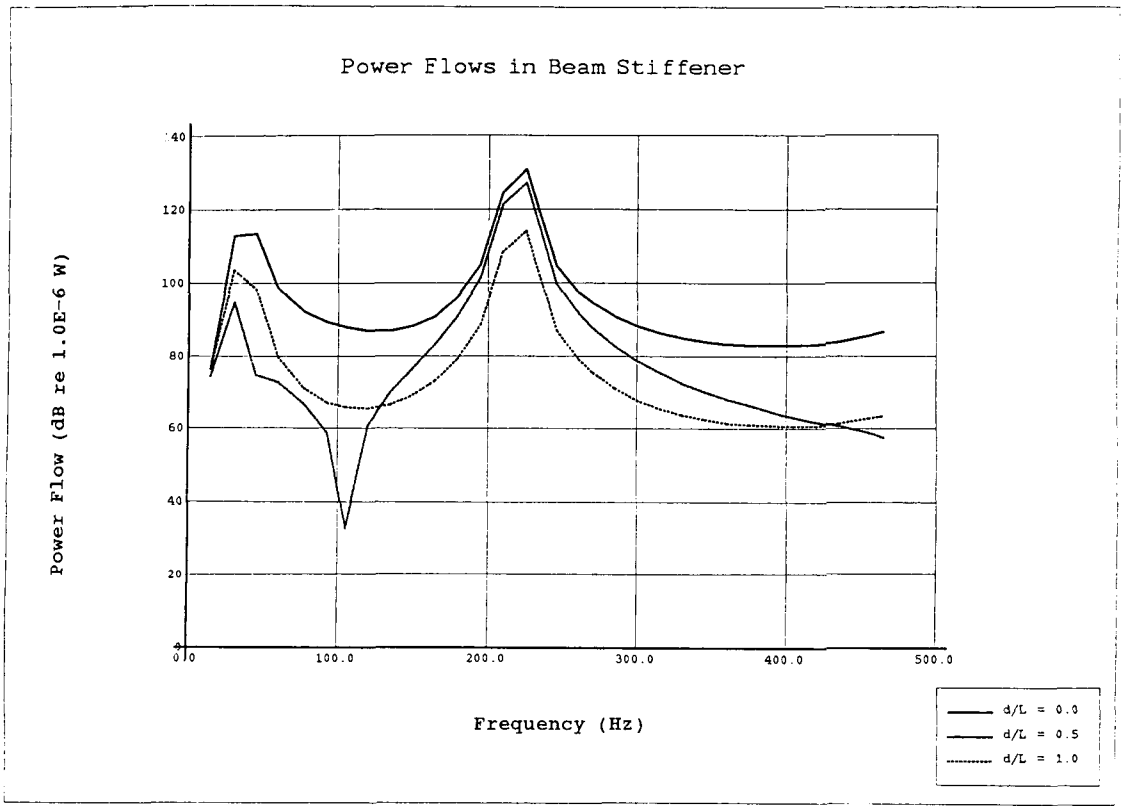

Fig. 10. Power Flows for Three Locations Along Beam Stiffener

For a plate element problem, spectrum plots are more difficult to generate and understand. Graphical (contour and vector) plots are needed to show the spatial variation of the power flow variables. A contour plot of the power flow magnitudes of the plate and beam elements is in Fig. 11. The beam elements are illustrated as plates in the diagram so their results may be visualized. Fig. 11 shows how power flows through the model at 455 Hz. Power flows into the model at the load points at the end of the plate, where some of it channels down the beam stiffeners, and the rest flows through the plate.

Fig. 12 shows a vector plot of power flow, which shows the directions that the power is flowing. The lengths of the arrows shorten as power travels from load point to the mountings at the end of the plate. In this case, almost all the power dissipated is due to material damping.

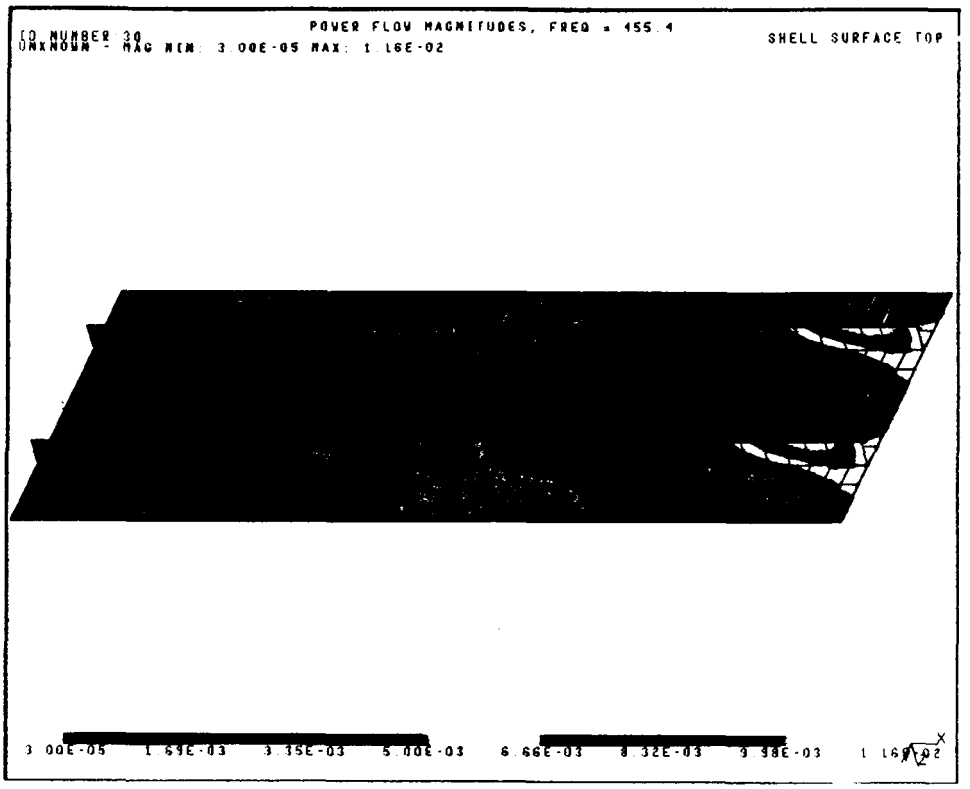

Fig. 11. Power Flow Magnitudes, f=455 Hz.

The effects of material damping are shown in Fig. 13, which is a plot of power dissipation. As mentioned in the "Damping and Power Dissipation" section earlier, a power dissipation field will resemble a mode shape, since dissipations are directly related to the squares of the displacements. In this case, the largest power sinks are outside the beam stiffeners and toward the rear of the plate.

Power balances are reasonably accurate for all frequencies, with the total power dissipations of the beam and plate elements matching the differences between input and output powers. The results show that both element types may be used accurately in a single model.

SUMMARY AND FUTURE WORK

A general capability for the calculation of power flow variables (power flow, mechanical intensity, power dissipation, power input and power output) has been developed for use with the finite elememt code NASTRAN. BAR, QUAD2, QUAD4, HEXA2, IHEXi, MASSi, and ELASi element types are currently supported. Unlike most of the studies presented in the literature, all types of power flows, flexural, axial, and torsional, are considered in the

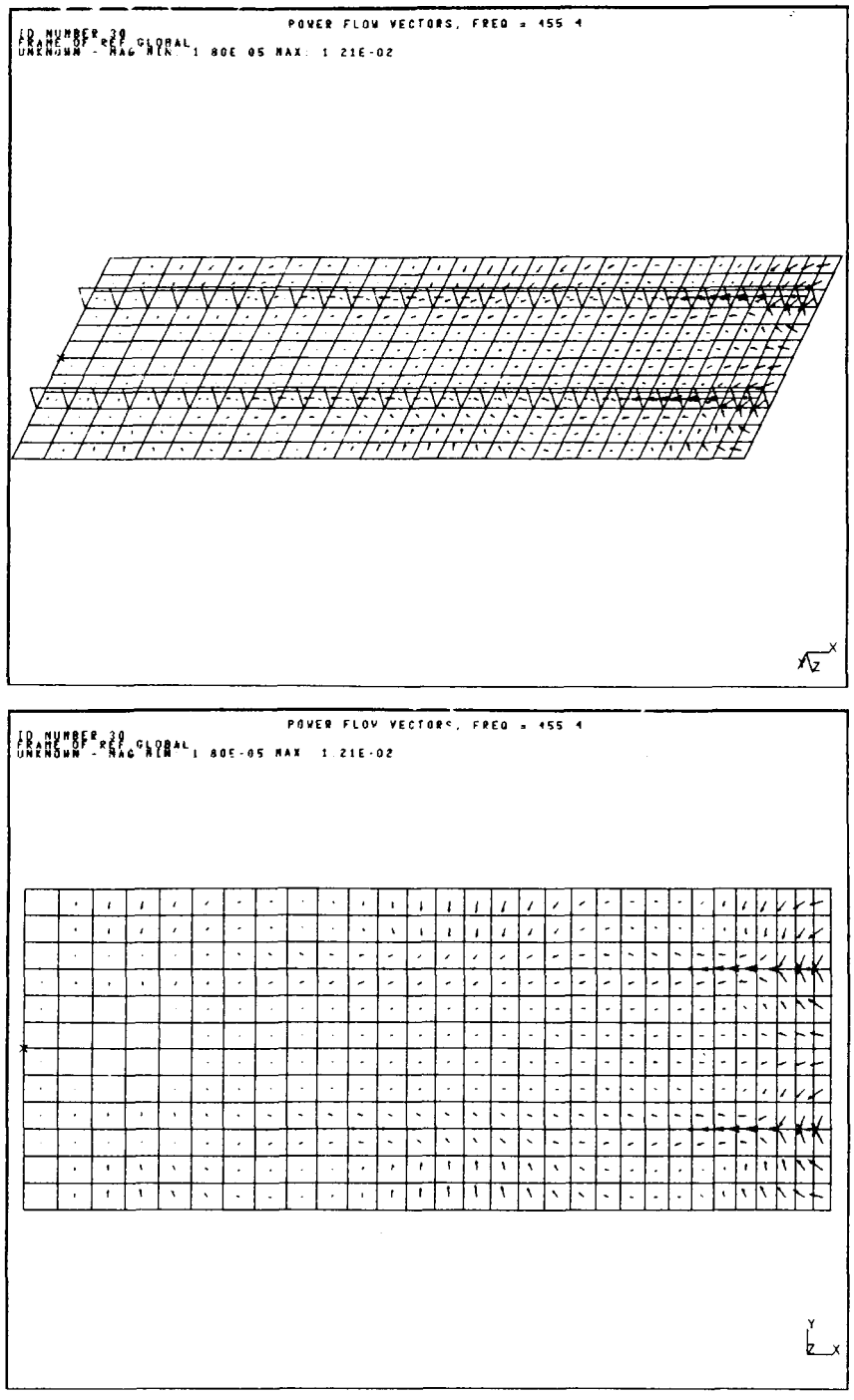

Fig. 12. Power Flow Directions (two views), f=455 Hz..

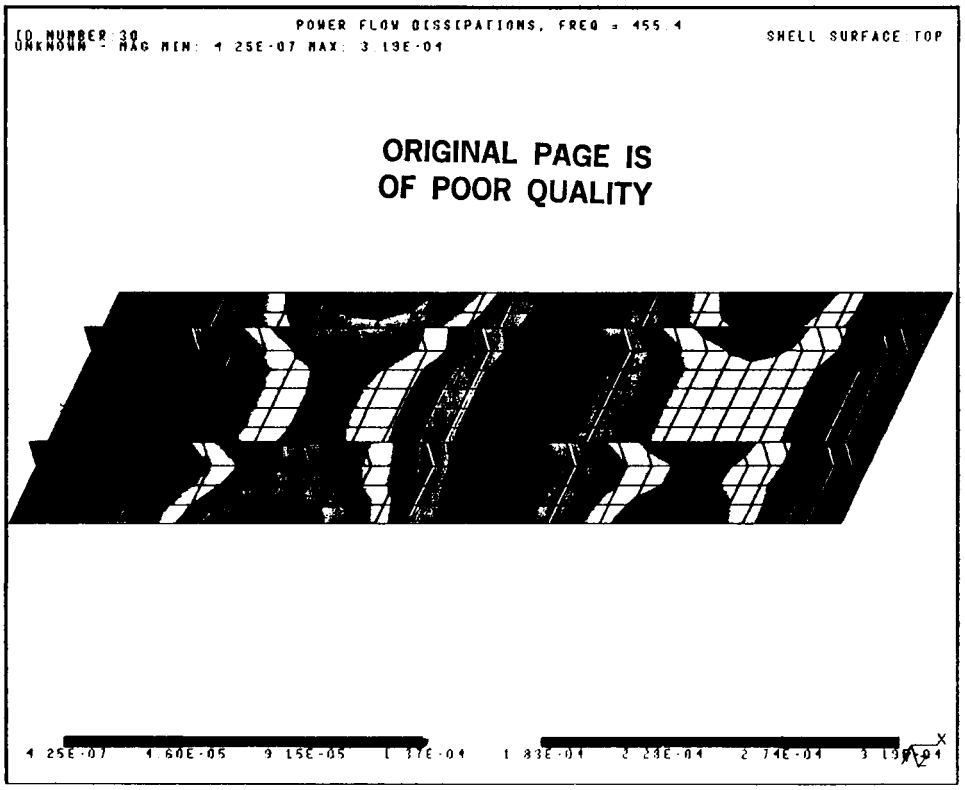

Fig. 13. Power Dissipations, f=455 Hz.

element formulations.

The results of the test problems indicate the method is a valid way of predicting the power flow response of a dynamically excited system at relatively low frequencies. Results for the test problems were more accurate at resonances than between resonances. Inaccuracies in the off-resonant responses are due to numerical problems; however, errors at low response are not as critical as errors at peaks.

Using FEA to calculate power flows is accurate and economical for the lower modes of a mechanical system. However the power flow results will only be as good as the NASTRAN results. Good modeling techniques and an understanding of the wavelength sizes of a problem are required. The shorter the wavelengths, the denser the required mesh will be.

Future work is extensive, and includes calculating power losses due to radiation damping, attaching dampers and active control devices to structures and measuring their effects, applying shape optimization techniques to structures with power flow variables as design constraints, determining the effects of mesh dependence, adding the power flow capability to NASTRAN, and developing a more specialized graphical post-processing package.

REFERENCES

1. Wohlever, J.C., and R.J. Bernhard, "Vibrational Power Flow Analysis of Rods and Beams," Report No. 0353-12 HL 88-24, Ray W. Herrick Laboratories, Purdue University, West Lafayette, Indiana (1988).

2. Luzzato, E., and E. Ortola, "The Characterization of Energy Flow Paths in the Study of Dynamic Systems using S.E.A. Theory," *Journal of Sound and Vibration,* Vol. 123, No. 1, pp. 189-197 (1988).

3. Rasmussen, G., "Structural Dynamic Measurements using Intensity Methods," Proceedings of the Third International Modal Analysis Conference, pp. 558-564 (1985).

4. Rasmussen, G., "Transducers for Structure Intensity Measurements," Proceedings of Inter-Noise '87, pp. 1183-1186 (1987).

5. Pavic, G., "Measurement of Structure-Borne Wave Intensity, Part 1: Formulation of the Methods," *Journal of Sound and Vibration,* Vol. 49, No. 2, pp. 221-230 (1976).

6. Pinnington, E.J., "Vibrational Power Transmission to a Seating of a Vibration Isolated Motor," *Journal of Sound and Vibration,* Vol. 118, No. 3, pp.515-530 (1987).

7. Pavic, G., "Structural Surface Intensity: An Alternative Approach in Vibration Analysis and Diagnosis," *Journal of Sound and Vibration,* Vol. 115, No. 3, pp. 405-422 (1987).

8. Lyon, R.L., *Statistical Energy Analysis of Dynamical Systems,* The M.I.T. Press, (1975).

9. Mickol, J.D., and R.J. Bernhard, "An Investigation of Energy Transmission Due to Flexural Wave Propagation in Lightweight, Built-Up Structures," Report No. 0353-4 HL 86-40, Ray W. Herrick Laboratories, Purdue University, West Lafayette, Indiana (1986).

10. Cuschieri, J., "Power Flow as a Complement to Statistical Energy Analysis and Finite Element Analysis," *Statistical Energy Analysis,* ASME, NCA-Vol. 3, edited by K.H. Hsu, D.J. Nefske, and A. Adnan (1987).

11. Nefske, D.J., and S.H. Sung, "Power Flow Finite Element Analysis of Dynamic Systems: Basic Theory and Application to Beams," *Statistical Energy Analysis,* ASME, NCA-Vol. 3, edited by K.H. Hsu, D.J. Nefske, and A. Adnan (1987).

12. "NASTRAN® User's Manual, NASA SP-222(08)," Computer Software Management and Information Center (COSMIC), University of Georgia, Athens, Georgia (1986).

13. Cremer, L., M. Heckl, and E.E. Ungar, *Structure-Borne Sound,* Springer-Verlag, New York (1973).

14. Noiseux, D.U., "Measurement of Power Flow in Uniform Beams and Plates," *Journal of the Acoustical Society of America,* Vol. 47, No. 1, pp. 238-247 (1970).

15. Verheij, J.W., "Cross Spectral Density Methods for Measuring Structure-Borne Power Flow on Beams and Pipes," *Journal of Sound and Vibration,* Vol. 70, No. 1, pp. 133-139 (1980).

16. Li, J., "The Propagation of the Bending Waves and Torsional Waves in a Combined Beam Structure," Proceedings of Inter-Noise '87, pp. 611-614 (1987).

17. Williams, E.G., H.D. Dardy, and R.G. Fink, "A Technique for Measurement of Structure-Borne Intensity in Plates," *Journal of the Acoustical Society of America,* Vol. 78, No. 6, pp. 2061-2068 (1985).

18. Koshiroi, T., and S. Tateishi, "Visualization of Vibration Energy Flow in Plates: Measurements of Vibrational Intensity," Proceedings of Inter-Noise '87, pp. 1375-1378 (1987).

19. Fahy, F.J., and R. Pierri, "Application of Cross-Spectral Density to a Measurement of Vibration Power Flow Between Connected Plates," *Journal of the Acoustical Society of America,* Vol. 62, No. 5, pp. 1297-1298 (1977).

20. Cuschieri, J.M., "Extension of Vibrational Power Flow Techniques to Two-Dimensional Structures," first annual report, grant number NAG-1-685 from NASA Langley Research Center, (Aug 1987).

21. "Supertab® Engineering Analysis Pre- and Post-Processing User Guide and Reference Manual," Structural Dynamics Research Corporation, Milford, Ohio (1986).

22. Heckl, M., "Examples of Structure-Borne Sound Visualization," Proceedings of Inter-Noise '87, pp. 603-606 (1987).

23. Nilsson, A.C., "Excitation and Propagation of Structure-Borne Sound in Ribbed Structures," Proceedings of Inter-Noise '84, pp. 547-552 (1984).